An Approach for Peg-in-Hole Assembling Based on Force Feedback Control

Peng Zou, Qiuguo Zhu, Jun Wu, Jianxiang Jin

pengzou@zju.edu.cn, qgzhu@zju.edu.cn, junwuapc@zju.edu.cn, jxjin@csc.zju.edu.cn

***Abstract*—In this paper, an intuitive and effective method is proposed for a sensor guided industrial robot to carry out the Peg-in-Hole assembly. This method contains two main steps. The first step is calibrating the wrist force sensor to compensate the load gravity and the bias of sensor so that the external force on the load can be precisely obtained. Secondly an impedance controller is designed to realize the compliant behavior between the manipulator and external environment. Different from the traditional method based on the position control loop, the force control strategy is based on the robot end-effector velocity control loop, which is easier and convenient to implement. Finally, a Peg-in-Hole experiment using an industrial manipulator with wrist sensor and a Peg-in-Hole mould with a tiny clearance was successfully completed. The experimental results verified the effectiveness and practicability of the proposed method.**

Keywords — Peg-in-Hole, sensor calibration, gravity compensation, impedance control

I. INTRODUCTION

Peg-in-Hole assembly as the most universal task of robotic assembly has been widely studied and applied in various fields from small-scale object assembly, such as electronic components [1], mold casting manufacturing [2], and even microproduct [3] assembly to large-scale components, such as aviation components [4], engines [5] and windshields assembly. However, it is still hard to find a practical and convenient approach in today's real industrial scenarios for many Peg-in-Hole tasks. This is mainly due to the inherent shortcomings of process, sensing, and control systems, which inevitably accompany contact with constrained surfaces, resulting in the occurence of reaction forces. Due to the peg and hole's high rigidity, even a slight error in the position/orientation will produce a big contact force, consequently, failure of operation. Many researchers use the vision sensors to overcome the uncertainty of position and orientation during the task.Huang et al. [6] and Chang et al. [3] presented position-based visual servo systems based on the image calibration method to complete the Peg-in-Hole task. Yoshimi et al. [7] proposed an operation algorithm for Peg-in-Hole mating based on image features of an uncalibrated camera to match the orientation and position between the peg and the hole.

Although position controller based on vision sensors has high precision, it may encountered some problems, such as large contact force due to the pose error or partial occlusion. Therefore, a force feedback control strategy can be introduced not only to detect the external force and guarantee the safe assembly process, but also to accommodate the position uncertainty. Two basic groups of force control methods can be distinguished: passive compliance and active compliance. In passive control, due to the inherent flexibility of the manipulator structure, servo mechanism or special compatible equipments, the position of the end effector is adjusted by the contact force itself. Remote center compliance, for example, is used to reduce assembly forces and allow pegs rotate freely [8]. However, the design of passive compliance in industrial fileds lacks flexibility because a dedicated compliant end effector must be designed and installed for each robotic task. For active control, the compliance of robot systems is mainly ensured by specially designed control systems. This method usually requires measuring contact forces and torques and feeding them back to the controller, which is used to modify or even generate the required trajectory of the robot's end effector online. Usually, the force/torque sensor is installed on the wrist joint, but there are other strategies, for example, the force sensor can be mounted on the fingertip of the robot hand. Similarly, external forces and moments can be estimated from the torque measurement of the joint torque sensor [9]. However, most applications of force control, including industrial fileds, are applying wrist force/torque sensors. In this case, it is neccessary that the weight and inertia of the tool installed between the sensor and the environment such as the robot end-effector shoud be compensated from the force/torque measurement. Son et al. [10] proposed a neural network structure to avoid jamming during peg insertion based on a wrist sensor. Shirinzadeh et al. [11] developed a comprehensive research of cylindrical peg-in-hole tasks for industrial robot. Newman et al. [12] designed a force torque mapping containing force and moment values in every contact point to finish assembly task. Although many researchers utilize the force sensor to overcome the uncertainty of the object position or orientation and execute the assembly task successfully, most of them did not describe

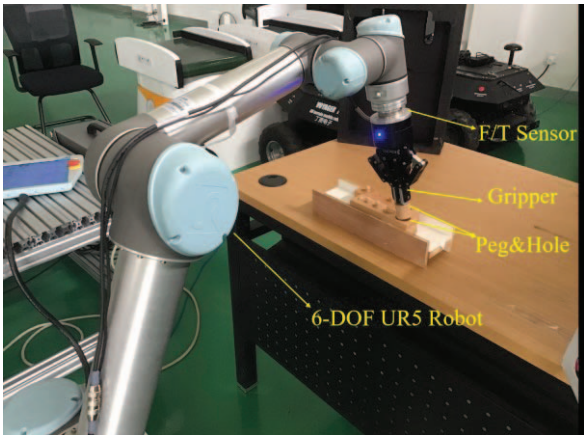

Fig. 1. Peg-in-Hole assembly system

This work was supported by State Key Laboratory of Industrial Control Technology (ITC1904).

Peng Zou, Qiuguo Zhu, Jun Wu, Jianxiang Jin are with the State Key Laboratory of Industrial Control and Technology, Zhejiang University, Hangzhou, P. R. China, Institute of Cyber-System and Control, Zhejiang University.

Qiuguo Zhu is the corresponding author. qgzhu@zju.edu.cn.

the sensor calibration method or control algorithm in detail. Moreover, their methods are too complicated to apply to industrial tasks. In this paper, a detailed force control strategy for the Peg-in-Hole assembly work is proposed, which is easy to implement and practical in real industrial fields. And a Peg-in-Hole experiment is also performed to test the effectiveness and practicability of the proposed method.

II. PEG-IN-HOLE APPROACH

In this section, the Peg-in-Hole approach is introduced detailly. Firstly, we give an brief introduction to the whole robotic Peg-in-Hole assembly system. Secondly, we propose a comprehensive sensor calibration method to compensate the influence of the load gravity and bias of sensor so that the external force on the peg can be precisely obtained. Thirdly, a force control frame is designed to compensate the uncertainty of the position and realize the robot compliant behavior when interacting the environment during the peg insertion process.

A. Robotic Peg-in-Hole Assembly System

Our experimental platform is shown in Fig. 1, which contains three components: pegs and holes, force sensor and a industrial 6-DoF robot with gripper. The robot used in this task is Universal Robots (UR5), which is equipped with a Robotiq 2F-85 gripper. An ATI force-torque(FT) sensor is placed between the robot and the Robotiq gripper. By writing python socket scripts in our own computer, we can control the robot and gripper via TCP/IP protocol. The pieces of force and torque information from force-torque sensor are read by communicating with the ATI NETBOX via UDP programming. In general, Peg-in-Hole task is that the robot inserts the pegs into the fixed hole according to the force feedback information from the force-torque sensor.

B. Sensor Calibration Method

Since the force sensor is installed between the wrist joint and the load, the force and torque values measured by the sensor during the assembly process consists of three parts: the bias of the sensor, the gravity of the load and the external contact force . In order to obtain the external force on the load, it is necessary to eliminate the influence of the sensor bias and load gravity. In this paper, we present a comprehensive identification method considering the bias of the sensor, installing angle of the sensor ,the gravity of the load and the centroid coordinate of the load to compensate the load gravity and the bias of sensor. As shown in Fig. 2, establishing the coordinate schematic diagram firstly.{B} and {W} represent the base frame and the wrist frame of the robot respectively.{S} denotes the sensor measurement frame. p is the centroid position and G is the tool gravity. The calibration method is as follows:

1) Centroid coordinate identification: The bias of the sensor can be expressed as $F_{x0}, F_{y0}, F_{z0}, M_{x0}, M_{y0}, M_{z0}$ and the force/torque values measured by force sensor can be marked as $F_x, F_y, F_z, M_x, M_y, M_z$. The tool gravity force vector consists of a force and a torque component is expressed relative to {S} as:

$$\begin{cases} G_x = F_x - F_{x0} \\ G_y = F_y - F_{y0} \\ G_z = F_z - F_{z0} \\ M_{gx} = M_x - M_{x0} \\ M_{gy} = M_y - M_{y0} \\ M_{gz} = M_z - M_{z0} \end{cases} \tag{1}$$

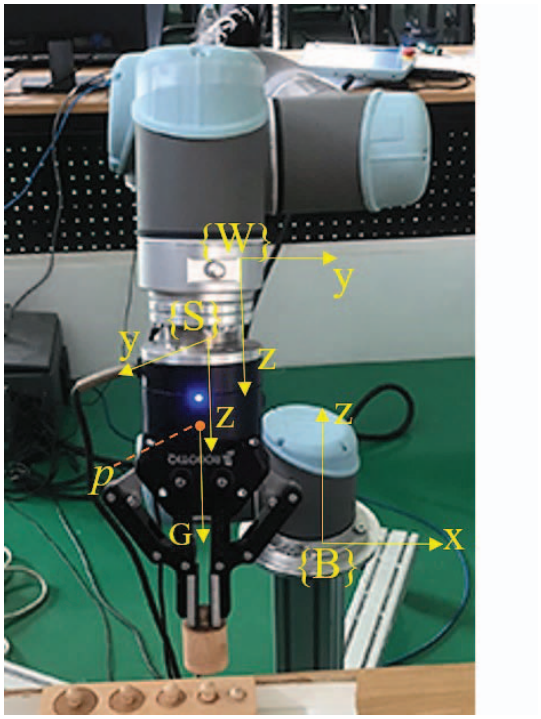

Fig. 2. Schematic diagram for definition of the coordinates

According to the relationship between force and torque:

$$\begin{cases} M_{gx} = G_z \times y - G_y \times z \\ M_{gy} = G_x \times z - G_z \times x \\ M_{gz} = G_y \times x - G_x \times y \end{cases} \tag{2}$$

where x, y, z represent the load centroid position p in {S}, substitute (1) in (2):

$$\begin{cases} M_x = F_z \times y - F_y \times z + M_{x0} + F_{y0} \times z - F_{z0} \times y \\ M_y = F_x \times z - F_z \times x + M_{y0} + F_{z0} \times x - F_{x0} \times z \\ M_z = F_y \times x - F_x \times y + M_{z0} + F_{x0} \times y - F_{y0} \times x \end{cases} \tag{3}$$

where $F_{x0}, F_{y0}, F_{z0}, M_{x0}, M_{y0}, M_{z0}, x, y, z$ are all constant, let

$$\begin{cases} k_1 = M_{x0} + F_{y0} \times z - F_{z0} \times y \\ k_2 = M_{y0} + F_{z0} \times x - F_{x0} \times z \\ k_3 = M_{z0} + F_{x0} \times y - F_{y0} \times x \end{cases} \tag{4}$$

Substitute (4) in (3):

$$\begin{bmatrix} M_x \\ M_y \\ M_z \end{bmatrix} = \begin{bmatrix} 0 & F_z & -F_y & 1 & 0 & 0 \\ -F_z & 0 & F_x & 0 & 1 & 0 \\ F_y & -F_x & 0 & 0 & 0 & 1 \end{bmatrix} \begin{bmatrix} x \\ y \\ z \\ k_1 \\ k_2 \\ k_3 \end{bmatrix} \tag{5}$$

Collecting N (N>=3) sets of data in different orientation and position:

$$\begin{bmatrix} M_{x1} \\ M_{y1} \\ M_{z1} \\ M_{x2} \\ M_{y2} \\ M_{z2} \\ \vdots \\ M_{xN} \\ M_{yN} \\ M_{zN} \end{bmatrix} = \begin{bmatrix} 0 & F_{z1} & -F_{y1} & 1 & 0 & 0 \\ -F_{z1} & 0 & F_{x1} & 0 & 1 & 0 \\ F_{y1} & -F_{x1} & 0 & 0 & 0 & 1 \\ 0 & F_{z2} & -F_{y2} & 1 & 0 & 0 \\ -F_{z2} & 0 & F_{x2} & 0 & 1 & 0 \\ F_{y2} & -F_{x2} & 0 & 0 & 0 & 1 \\ & & \vdots & & & \\ 0 & F_{zN} & -F_{yN} & 1 & 0 & 0 \\ -F_{zN} & 0 & F_{xN} & 0 & 1 & 0 \\ F_{yN} & -F_{xN} & 0 & 0 & 0 & 1 \end{bmatrix} \begin{bmatrix} x \\ y \\ z \\ k_1 \\ k_2 \\ k_3 \end{bmatrix} \tag{6}$$

Which is:

$$m = F \cdot p \tag{7}$$

According to the least square method:

$$p = (F^T F)^{-1} \cdot F^T m \tag{8}$$

So we get the centroid coordinate of the load and constant k_1, k_2, k_3.

2) Sensor's installing angle and bias computation: As shown in Fig. 2, the sensor frame {S} is not parallel to the wrist frame {W}. It is assumed that the frame {S} can be rotated around the Z axis of the frame {W} by an angle θ.So the frame {W} denoted in the frame {S} by the rotation matrix is:

$$^S_W R = \begin{bmatrix} cos\theta & sin\theta & 0 \\ -sin\theta & cos\theta & 0 \\ 0 & 0 & 1 \end{bmatrix} \tag{9}$$

The tool gravity vector can be denoted relative to the base frame {B} as:

$$g_t = (0,0,-G)^T \tag{10}$$

Then the tool gravity vector denoted in the frame{S} can be got by the transformation matrix:

$$g_t^S = {}^S_W R \cdot {}^W_B R \cdot g_t \tag{11}$$

where $^W_B R$ is the rotation matrix from the wrist frame to the base frame, which can directly obtained from the robot controller in real time .Before the robot contact the environment, the force values measured by the sensor equal the tool gravity plus the bias of the sensor:

$$g_t^S + F_d^S = F^S \tag{12}$$

which is:

$$\begin{bmatrix} cos\theta & sin\theta & 0 \\ -sin\theta & cos\theta & 0 \\ 0 & 0 & 1 \end{bmatrix} \begin{bmatrix} r_{11} & r_{12} & r_{13} \\ r_{21} & r_{22} & r_{23} \\ r_{31} & r_{32} & r_{33} \end{bmatrix} \begin{bmatrix} 0 \\ 0 \\ -G \end{bmatrix} + \begin{bmatrix} F_{x0} \\ F_{y0} \\ F_{z0} \end{bmatrix} = \begin{bmatrix} -Gcos\theta r_{13} - Gsin\theta r_{23} \\ Gsin\theta r_{13} - Gcos\theta r_{23} \\ -Gr_{33} \end{bmatrix} + \begin{bmatrix} F_{x0} \\ F_{y0} \\ F_{z0} \end{bmatrix} = F^S = \begin{bmatrix} F_x \\ F_y \\ F_z \end{bmatrix} \tag{13}$$

Rewriting (13), we can get

$$\begin{bmatrix} -r_{13} & -r_{23} & 0 \\ -r_{23} & r_{13} & 0 \\ 0 & 0 & -r_{33} \end{bmatrix} \begin{bmatrix} Gcos\theta \\ Gsin\theta \\ G \end{bmatrix} + \begin{bmatrix} F_{x0} \\ F_{y0} \\ F_{z0} \end{bmatrix} = \begin{bmatrix} F_x \\ F_y \\ F_z \end{bmatrix} \tag{14}$$

where r_{13}, r_{23}, r_{33} are the third column values of $^W_B R$,which is known constant, rewrite (14):

$$\begin{bmatrix} -r_{13} & -r_{23} & 0 & 1 & 0 & 0 \\ -r_{23} & r_{13} & 0 & 0 & 1 & 0 \\ 0 & 0 & -r_{33} & 0 & 0 & 1 \end{bmatrix} \begin{bmatrix} Gcos\theta \\ Gsin\theta \\ G \\ F_{x0} \\ F_{y0} \\ F_{z0} \end{bmatrix} = \begin{bmatrix} F_x \\ F_y \\ F_z \end{bmatrix} \tag{15}$$

Similar to (5) and (6) ,we obtain:

$$f = R \cdot u \tag{16}$$

According to the least square method:

$$u = (R^T R)^{-1} \cdot R^T f \tag{17}$$

where:

$$u = \begin{bmatrix} Gcos\theta & Gsin\theta & G & F_{x0} & F_{y0} & F_{z0} \end{bmatrix} \tag{18}$$

So the force bias of the sensor and the tool gravity G are known. Then , according to (4) and (18):

$$\begin{cases} \theta = arccos\left(\frac{Gcos\theta}{G}\right) or \ \theta = arcsin\left(\frac{Gsin\theta}{G}\right) \\ M_{x0} = k_1 - F_{y0} \times z + F_{z0} \times y \\ M_{y0} = k_2 - F_{z0} \times x + F_{x0} \times z \\ M_{z0} = k_3 - F_{x0} \times y + F_{y0} \times x \end{cases} \tag{19}$$

As so far, all bias of the sensor, installing angle of the sensor, the gravity of the load and the centroid coordinate of the load are all known.

3) External force computation: The external force on the load during the peg insertion can be expressed in the frame {S} as:

$$\begin{cases} F_{ex} = F_x - F_{x0} - G_x \\ F_{ey} = F_y - F_{y0} - G_y \\ F_{ez} = F_z - F_{z0} - G_z \\ M_{ex} = M_x - M_{x0} - M_{gx} \\ M_{ey} = M_y - M_{y0} - M_{gy} \\ M_{ez} = M_z - M_{z0} - M_{gz} \end{cases} \tag{20}$$

where

$$\begin{cases} G_x = -Gcos\theta r_{13} - Gsin\theta r_{23} \\ G_y = Gsin\theta r_{13} - Gcos\theta r_{23} \\ G_z = -Gr_{33} \end{cases} \tag{21}$$

and M_{gx}, M_{gy}, M_{gz} can be computed by (2). After compensating the load gravity and the bias of the sensor ,the precise external force on the load is obtained.

C. Force Control Method

After getting the external force feedback information, we can use force control strategy to control the interact force

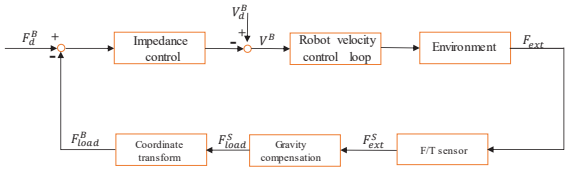

Fig. 3. Whole force control system based on robot end-effector velocity control loop

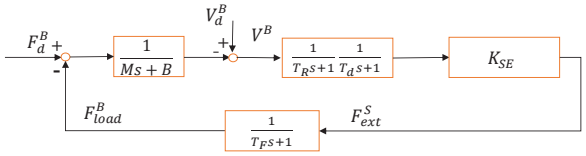

Fig. 4. Force control transfer function block diagram

between the peg and the hole. In this paper, we choose position-based impedance control [13] as our force control method. Impedance control is a common method for contact task , where the robot dynamic behavior is like a mass-spring-dashpot system. The impedance control law is shown in (22):

$$F_d - F = M_d(\dot{V}_d - \dot{V}) + B_d(V_d - V) \tag{22}$$

where M_d, B_d are diagonal positive definite matrices which define the target inertial and damping. $\dot{V}_d, \dot{V}$ denote the desired and actual robot Cartesian velocity vector and F_d, F denote the desired and actual external force vector respectively. The spring stiffness term is omitted because the restoring forces is not necessary for the assembling task. As shown in Fig. 3, the impedance controller implements the conversion of the force error signal to a velocity error signal. Obviously, this method is very convenient and easy to implement in industrial robots since it is based on the robot conventional velocity controller and does not require any modification of the robot original control system. Next, we will focus on the static characteristics of the presented system.

The transfer function block diagram is shown in Fig. 4, where T_R denotes the rise time of the inertial element of the robot velocity control system, T_d denotes the delay time of the velocity control system, T_F denotes the filter time constant,K_{SE} denotes the stiffness of the environment. In the Peg-in-Hole task, the desired velocity $\dot{V}_d$ is 0. So the closed-loop transfer function of the entire control system is:

$$\emptyset(s) = \frac{(T_F s+1)K_{SE}}{(Ms+B)(T_R s+1)(T_d s+1)(T_F s+1)+K_{SE}} \tag{23}$$

We can select appropriate M and B to make the system stable based on the routh stability criterion. The error of the system is

$$\begin{gathered} \text{let: } G_F(s) = 1/(T_F s + 1) \\ E(s) = F_d(s) - F_{ext}(s)G_F(s) = \\ F_d(s) - F_d(s)\emptyset(s)G_F(s) = \\ F_d(s)[1 - \emptyset(s)G_F(s)] \end{gathered} \tag{24}$$

The steady-error of the system is:

$$e_{ss} = \lim_{s\to 0} sE(s) = \lim_{s\to 0} sF_d(s)[1 - \emptyset(s)G_F(s)] \tag{25}$$

When the input is step signal:

$$\begin{aligned} e_{ss} &= \lim_{s\to 0} sF_d(s)[1 - \emptyset(s)G_F(s)] \\ &= \lim_{s\to 0} s \cdot \frac{1}{s}\left[1 - \frac{K_{SE}}{B+K_{SE}}\right] = \frac{B}{B+K_{SE}} \end{aligned} \tag{26}$$

In general, $K_{SE} \gg B$, so e_{ss} is approximately 0.

III. Experimental Results

A. Experiment Design

As Fig. 1 is shown, an industrial robot UR5 with 6-DOF containing a F/T sensor type ATI min45 and a Robotiq 2F-85 gripper is used in the experiment. The peg and hole are shown in Fig. 5(b), both of them are made of wood and their clearance is 0.1mm. The Peg-in-Hole task can be decomposed into three major phases as shown in Fig. 5(a): (1) Approaching Phase, (2) Orientation Adjustment Phase, (3) Insertion Phase. In this paper, we only focus on the latter two. So we use the position control to make the peg approach the hole with a small pose error firstly and then the impedance control mentioned above is applied during the next two phases.

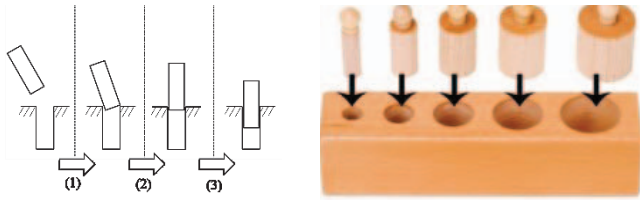

(a) (b)

Fig. 5. (a)Three phase during Peg-in-Hole (b)Peg and Hole

B. Experimental Results

1) Gravity compensation results: Use the sensor calibration and computation method presented in section II-B, we can identify the bias of the sensor, installing angle of the sensor, the gravity of the load and the centroid coordinate of the load and then compensate the bias of the sensor and the tool gravity. The force and torque values measured by the sensor before and after compensation is shown in Fig. 6. Apparently, the force and torque values are all almost 0 after compensation, which proves that our method has a high accuracy.

2) Peg-in-Hole task results: The assembly task was successfully executed as shown in Fig. 8.The robot firstly grasped the peg from free state to contact state by position control until peg contacts the hole's internal surface .Then we use the impedance controller mentioned in section II-C to control the contact force during the task. Set reference force F_d = [0,0,10,0,0,0] , V_d = [0,0,0,0,0,0] M= [1,1,1,0.1,0.1,0.1] , B=[160,160,160,6,6,6] . The real-time force and torque values read from the sensor during the whole assembling task is shown in Fig. 7. We can see that in the end of the approaching phase ,the contact force F_z increases to 76 N because of the pose error. Then it moves on to the orientation adjustment phase and the peg is rotated by the impedance controller to align the peg parallel to the hole. Finally, the forces and torques in all directions are decreased to about 0.Then it comes to the insertion phase, we still use the impedance controller to adjust the peg's orientation to control the interact force between the peg and the hole. As depicted in Fig. 7, the forces and torques are all almost 0 in the insertion process,which shows that the impedance

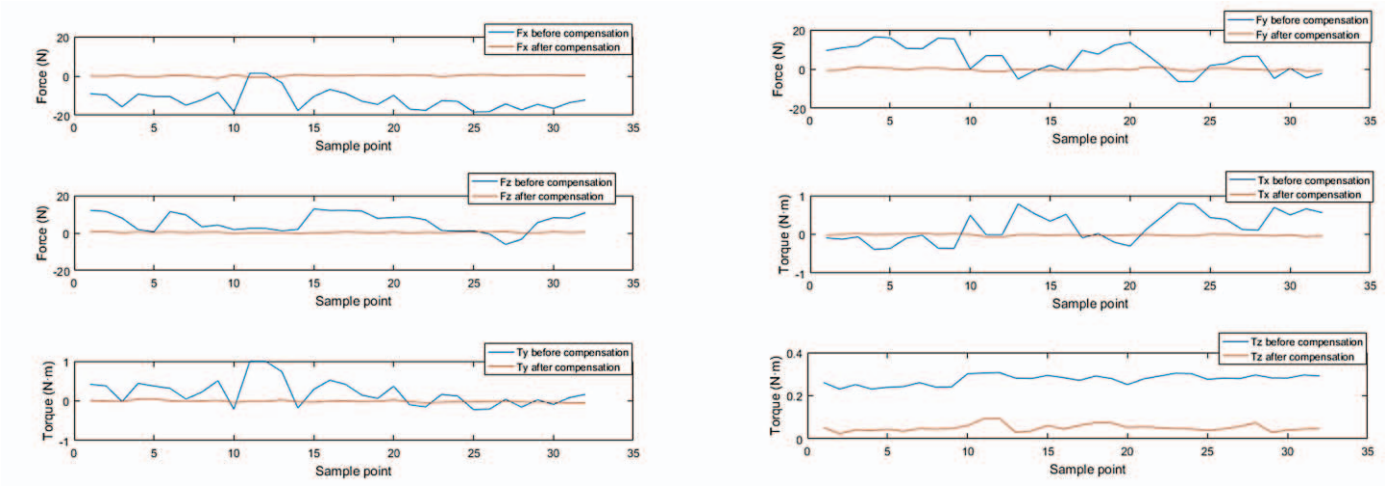

Fig. 6. Force and torque values before and after compensation

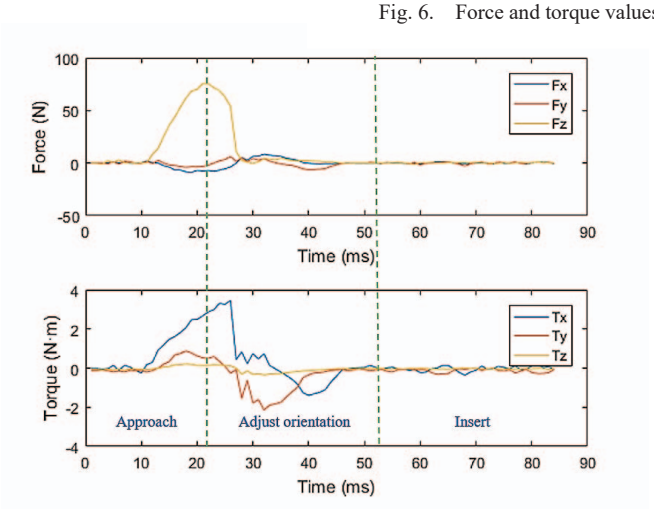

Fig. 7. Force and torque measurements in the task

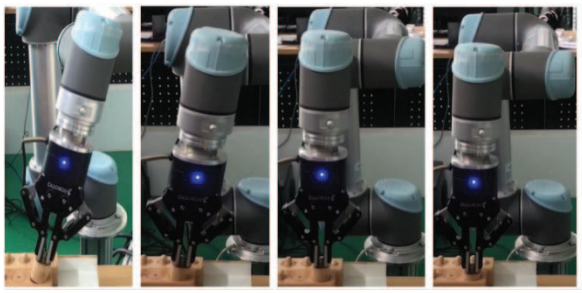

Fig. 8. A snapshot of the Peg-in-Hole processing

controller can realize the compliant interaction from the peg and the hole without jamming in the insertion phase.

IV. Conclusion

In this paper, an intuitive and effective force control strategy is proposed for the Peg-in-Hole assembling task. The strategy contains two main steps. The first step is to calibrate the wrist force sensor to compensate the load gravity and the bias of sensor so that the external force on the load can be precisely obtained. The second step is to design an impedance controller to yield compliant behavior without jamming during the task. Finally, a Peg-in-Hole experiment is successfully implemented based on the proposed method, which verifies the effectiveness of the approach. What is more, the method has a good engineering application value since it is simple to implement and practicable for real industrial tasks.

References

[1] J. Su, H. Qiao, Z. Ou, and Y. Zhang, "Sensor-less insertion strategy for an eccentric peg in a hole of the crankshaft and bearing assembly,"Assembly Automation, vol. 32, no. 1, pp. 86–99, 2012.

[2] P. Nagarajan, S. S. Perumaal, and B. Yogameena, "Vision based pose estimation of multiple peg-in-hole for robotic assembly," in International Conference on Computer Vision, Graphics, and Image processing.Springer, pp. 50–62,2016.

[3] R. Chang, C. Lin, and P. Lin, "Visual-based automation of peg-in-hole microassembly process," Journal of Manufacturing Science and Engineering, vol. 133, no. 4, p. 041015, 2011.

[4] A. Wan, J. Xu, H. Chen, S. Zhang, and K. Chen, "Optimal path planning and control of assembly robots for hard-measuring easy-deformation assemblies," IEEE/ASME Transactions on Mechatronics, vol. 22, no. 4,pp. 1600–1609, 2017.

[5] J. Su, H. Qiao, C. Liu, and Z. Ou, "A new insertion strategy for a peg in an unfixed hole of the piston rod assembly," The International Journal of Advanced Manufacturing Technology, vol. 59, no. 9-12, pp. 1211–1225, 2012.

[6] S. Huang, Y. Yamakawa, T. Senoo, and M. Ishikawa, "Realizing peg-and-hole alignment with one eye-in-hand high-speed camera," in Advanced Intelligent Mechatronics (AIM), 2013 IEEE/ASME International Conference on. IEEE, pp. 1127–1132, 2013.

[7] B.H. Yoshimi, P.K. Allen, "Active, uncalibrated visual servoing", IEEE International Conference on in Robotics and Automation (ICRA), San Diego, CA, pp. 156-161,1994.

[8] A.Romiti, G.Belforte, N.D'Alfio and F. Quagliotti, "A passive assembly device for the speedy assembly of pegs in holes", Assembly Automation, Vol. 1 No. 3, pp. 156-160,1981.

[9] J.Y.S.Luh, W.D.Fisher, R.P.C. Paul: Joint torque control by direct feedback for industrial robots, IEEE Trans. Autom. Contr. 28, 153–161,1983.

[10] C.Son, "A neural/fuzzy optimal process model for robotic part assembly", International Journal of Machine Tools and Manufacture, Vol. 41 No. 12, pp. 1783-1794,2001.

[11] B. Shirinzadeh, Y. Zhong, P. D. W. Tilakaratna, Y. Tian, and M. M.Dalvand, "A hybrid contact state analysis methodology for robotic-based adjustment of cylindrical pair," Int. J. Adv. Manuf. Technol., vol. 52, no. 1,pp. 329–342, 2011.

[12] W. S. Newman, Y. Zhao, and Y.-H. Pao, "Interpretation of force and moment signals for compliant peg-in-hole assembly," in Proc. IEEE Int.conf. Robot. Autom., pp. 571–576,2001.

[13] N. Hogan, "Impedance control: An approach to manipulation: Part I theory; part II implementation; part III applications," J. Dyn. Sys.,Meas., Control, vol. 107, no. 12, pp. 1–24, 1985.